Journal of Maps

ISSN: 1744-5647 (Online) Journal homepage: www.tandfonline.com/journals/tjom20

# Geology of the central Kohistan Arc, Northern Swat, Kalam (NW, Pakistan), results of a new 1:50,000 scale geological mapping

Tanveer Ahmad, M. Qasim Jan & Kirsten Drüppel

**To cite this article:** Tanveer Ahmad, M. Qasim Jan & Kirsten Drüppel (2025) Geology of the central Kohistan Arc, Northern Swat, Kalam (NW, Pakistan), results of a new 1:50,000 scale geological mapping, Journal of Maps, 21:1, 2572765, DOI: 10.1080/17445647.2025.2572765

**To link to this article:** https://doi.org/10.1080/17445647.2025.2572765

JOURNAL OF MAPS
2025, VOL. 21, NO. 1, 2572765
https://doi.org/10.1080/17445647.2025.2572765

SCIENCE

OPEN ACCESS Check for updates

# Geology of the central Kohistan Arc, Northern Swat, Kalam (NW, Pakistan), results of a new 1:50,000 scale geological mapping

Tanveer Ahmad[a], M. Qasim Jan[b,c] and Kirsten Drüppel[a]

[a]Institute for Applied Geosciences, Karlsruhe Institute for Technology (KIT), Karlsruhe, Germany; [b]National Centre of Excellence in Geology, University of Peshawar, Peshawar, Pakistan; [c]China-Pakistan Joint Research Centre on Earth Sciences, Islamabad, Pakistan

**ABSTRACT**

The study area in, northern Swat, Pakistan represents a critical segment of the Cretaceous to Tertiary Kohistan arc. It is characterized by complex interplay of plutonic, volcanic and metamorphic systems, whose magmatic and tectonic relationships remains poorly constrained. The study aims to elucidate the tectonomagmatic evolution of the central-western Kohistan Arc, by providing a new detailed geological map (Ahmad et al., 2025b), based on field work combined with petrographic observations, geochemical, structural and age data. The geological map also integrates previous field data, which was carefully revisited during recent field studies. Macroscopic observations and age relationships of the key lithological units are defined, revealing a magmatic sequence of late Cretaceous to mid-Eocene plutonic rock suites intruding Cretaceous (meta?) volcanic and metasedimentary rocks. Plutonic rocks of the study area comprise the late Cretaceous Matiltan and Bhankhwarh granites, mafic to intermediate Paleocene to Early Eocene plutons like the Smoky diorite, and the Gabral and Deshai quartz diorites and associated gabbroic dykes and plugs, followed by the younger mid-Eocene Diwanger quartz monzonite, Shahibagh granodiorite, and Jut Banda granite. The foliation of the wall rocks runs NE–SW and dips steeply toward the northwest. Minor faults and shear zones are also present in the plutonic rocks. The present study improves the understanding of the geological evolution of the northern Swat Kohistan Arc.

**ARTICLE HISTORY**
Received 28 July 2025
Revised 27 September 2025
Accepted 2 October 2025

**KEYWORDS**
Gabbroic rocks; granitoids; Kohistan Arc; plutonic rocks; tectonomagmatic evolution

## 1. Introduction

The Kohistan Arc (KA) in Pakistan is one of the most extensively studied island arcs, with numerous geological maps and models synthesizing its overall geology and tectonic settings. Early geological maps mostly deal with particular features of specific areas (Bard, 1983; Dhuime et al., 2009; Ivanac et al., 1956; Jan & Mian, 1971; ; Petterson, 2010; Petterson & Windley, 1985, 1991; Tahirkheli, 1979; Treloar et al., 1996). Despite the large amount of data available, the central-western KA, including the northern Swat-Kalam area, remains poorly detailed and under-explored due to limited accessibility, despite excellent exposure. This region hosts diverse lithologies—Late Jurassic to Late Cretaceous metasediments and volcanics, and Late Cretaceous to Mid-Eocene granitoids including granites, diorites, monzonites, granodiorites, and gabbros (Ahmad et al., 2025b; Jan & Mian, 1971). Recent work identifies two magmatic stages: Stage I (77–53 Ma) with calc-alkaline, arc-type characteristics, and Stage II (47–44 Ma) with high-potassic to shoshonitic affinities indicating a post-collisional setting (Ahmad et al., 2025b).

The large variety of the exposed rock units and their complex contact relationships require a detailed and thorough investigation of their spatial and temporal relationships, both in the field and in the laboratory, in order to provide an improved map of the area. The study area is of particular importance due to its lithological variety when compared to other parts of the KA, which provides key insights into specific magmatic episodes. The complexity and diversity of rock units necessitate detailed investigation of their spatial and temporal relationships to refine mapping and enhance understanding of the region's geology.

This study aims to characterize lithologies, delineate pluton extents and contacts, and clarify the geological and structural framework of the central KA. Mapping was conducted using toposheet 43A/6 (1:50,000), prior studies (Jan & Asif, 1983; Jan & Mian, 1971; Khalil & Afridi, 1979), and satellite imagery. Major transects followed the Ushu, Bhankhwarh, Gabral, and Shahibagh rivers. A new 1:50,000 geological map illustrates spatial and age relationships of Late Cretaceous to Mid-Eocene magmatic units and host rocks.

**CONTACT** Tanveer Ahmad tanveer.ahmad@kit.edu Institute for Applied Geosciences, Karlsruhe Institute for Technology (KIT), Adenauerring 20b, 76131 Karlsruhe, Germany

Supplemental data for this article can be accessed online at https://doi.org/10.1080/17445647.2025.2572765.

### 1.1. Objectives

The main objective of this work is to provide a precise and detailed geological map of the central-western Kohistan Arc, a region that has hardly been systematically mapped to date. In addition, the study aims to characterize the various exposed metamorphic, volcanic and plutonic rock units and to determine their contact and age relationships, in order to understand the tectonomagmatic framework of the central-western KA.

## 2. Geography and geomorphology of the study area

The Kalam study area is located in northern Swat District, NW Pakistan, between 35°30′–35°50′N latitude and 72°15′–72°45′E longitude, covering c. 50 km². Situated about 96 km from Mingora and accessible via a main road, Kalam is bordered by Chitral and Dir Kohistan to the north and south, Bahrain and Madyan to the east, and the Dir District to the west. The study area lies within the Hindukush mountain range. The terrain features east–west trending mountains up to 5000 meters above sea level, characterized by high relief, rugged landscapes, and deeply incised valleys. Steep cliffs and ice-covered, peaks dominate the skyline. U-shaped valleys with flat floors and steep sides reflect glacial erosion. The area's main drainage is through the Ushu and Gabral rivers, along with smaller tributaries, which significantly influence the region's geomorphology. Settlements are scattered along major valleys.

## 3. Regional geological setting

Northern Pakistan consists of three major tectonic domains (from south to north): the Indian Plate, the Kohistan Arc (KA), and the Karakoram microplate (southern part of the Eurasian Plate) (Searle et al., 1999; Tahirkheli, 1979) (Figure 1(a)). The Karakoram terrain, geologically equivalent to Tibet's Qiantang terrain, is bounded by the Rushan-Pshart Suture Zone to the north (Pamir) and the Shyok Suture (Main Karakoram Thrust, MKT) to the south, separating it from the Kohistan-Ladakh Arc (Searle, 2011). The Karakoram microplate includes three main units: (1) the northern sedimentary terrain, (2) the Karakoram Batholith, and (3) the southern metamorphic complex (Gaetani, 1997; Searle, 2011). Gaetani (1997) and Zanchi et al. (2000) further divided it into the northern Hindukush terrain and the southern Karakoram domain, joined along the Tirich Mir–Kilik Fault (Figure 1(a)).

The KA lies between the converging Indian and Asian plates, bounded by the MKT (north) and the Indus Suture Zone or Main Mantle Thrust (MMT) to the south (Burg, 2011; Jagoutz & Schmidt, 2012; Tahirkheli & Jan, 1979). The Indian Plate comprises Precambrian–Paleozoic crystalline and metasedimentary rocks, with a Late Paleozoic–Mesozoic cover of Lesser Himalayan rocks and Sub-Himalayan molasse (Searle et al., 1999; Ahmad et al., 2021a, 2021b). In addition, several carbonatites–alkaline complexes intrude the greater Himalayan sequence in the Peshawar Plain region, collectively termed the Peshawar Plain Alkaline Igneous Province that includes the Loe-Shilman, Sillai Pattai, Ambela, Shewa, Malakand and Koga Alkaline complexes (Kempe & Jan, 1970, Khan et al., 2025).

### 3.1. Kohistan arc (KA)

The KA (Figure 1(b)) is considered one of the most complete exposed crustal sections globally, from mantle-adjacent lower crust to upper crustal rocks (Bard, 1983; Burg, 2011; Petterson, 2010; Tahirkheli, 1979). In the Indus Valley, the KA is subdivided into seven east–west trending lithological units of Jurassic to Oligocene age, i.e. (from north to south), the Yasin Group, Chalt Volcanic Group, Jaglot Group, Kohistan Batholith, Chilas Complex, Kamila Amphibolites, and the Jijal–Sapat mafic-ultramafic complexes (Dhuime et al., 2009; Petterson & Windley, 1985; Treloar et al., 1996).

In the north, the Yasin Group metasediments and volcanics with Albian–Aptian fossils (Ivanac et al., 1956; Pudsey, 1986) overlie the Chalt Group basaltic to rhyolitic volcanics, tuffs, and pyroclastics of possible Lower Jurassic to Cretaceous age (Petterson & Windley, 1991). The Jaglot Group, composed of back-arc basin deposits (Thelichi, Gilgit, and Gashu formations), underlies Eocene volcanics of Dir-Kalam to the west (Khan et al., 1993; Khan et al., 1997). Both the Jaglot and Chalt groups are intruded by plutons of the Kohistan Batholith in the south (Petterson & Windley, 1985). The Kohistan Batholith is followed toward the south by the >250 km long and up to 40 km wide Chilas Complex, mainly composed of gabbronorite and minor ultramafic–mafic intrusions (Jan, 1979a; Khan et al., 1989; Khan et al., 1993). The Kamila Amphibolite Belt to the south consists of amphibolite-facies metagabbros, metadiorites, metatonalites, metavolcanics, and minor metasediments (Jan, 1988; Jan, 1979b; Treloar et al., 1990). The southern margin of the KA hosts partly layered mafic-ultramafic bodies, including the Tora Tiga, Jijal, Sapat, and Babuser complexes (Burg, 2011; Jan et al., 1993; Jan et al., 2025; Jan & Howie, 1981).

### 3.2. Kohistan Batholith

The Kohistan Batholith is an integral part of the KA, composed mainly of calc-alkaline granites, tonalites,

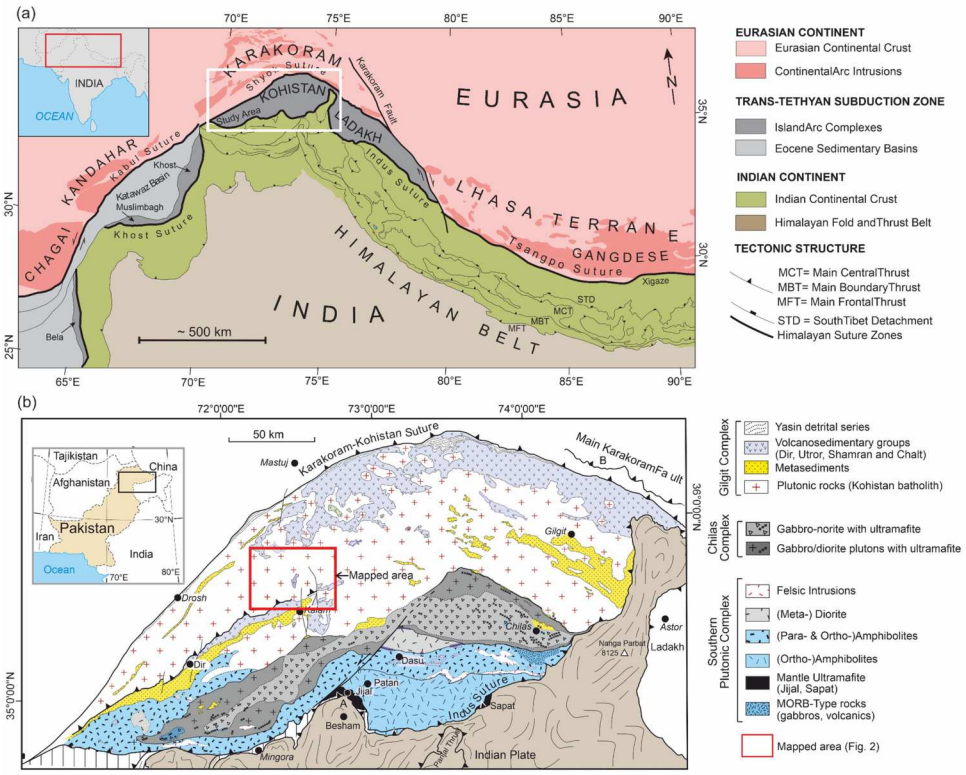


**Figure 1.** (a) Overview map of the tectonic framework of the Karakoram–Himalaya–Tibet orogenic system after Martin et al. (2020); b) Geological Map of the Kohistan Island Arc showing different lithological units (after Tahirkheli and Jan (1979), Searle et al. (1987), Dhuime et al. (2009), and Jagoutz and Schmidt (2012)). Red box shows location of the study area.

diorites, and minor gabbros, with diverse ages and compositions (Bouilhol et al., 2013; Jagoutz et al., 2006, 2018; Petterson, 2010; Ullah et al., 2025). Petterson and Windley (1985) and Kazmi and Jan (1997) identified three major intrusion phases: (1) an early (102 ± 12 Ma) bimodal suite of gabbro-diorite and tonalite, (2) a main magmatic phase with granitoids formed in an Andean-type margin (85–40 Ma), and (3) post-collisional leucogranites (30–26 Ma). Recent U–Pb zircon dating and isotopic studies show that calc-alkaline magmatism began in the Jurassic (c. 154 Ma) and continued into the Miocene (Bouilhol et al., 2013; Heuberger et al., 2007). These new data support the interpretation of the KA as a long-lived island arc that persisted until the India–Arc collision (c. 50 Ma) and the final India–Eurasia collision (c. 40 Ma) (Bouilhol et al., 2013).

## 4. Methods

Geological fieldwork in the northern Swat–Kalam region was conducted along four deeply incised river valleys from east to west: Ushu, Bhankhwarh, Gabral, and Shahibagh. Lithologies were primarily identified along these valleys, with the locations of their contacts being precisely recorded using a Garmin GPS. In addition, structural measurements were systematically collected. Extensions of lithologies into inaccessible, high-altitude areas were inferred from stream-transported boulders and landslide debris, then verified using satellite imagery via Google Earth and ArcMap. Data were plotted on the topographic map sheet 43A/6 (1:50,000; Survey of Pakistan), and the spatial dataset was subsequently incorporated into ArcGIS, where it was georeferenced, digitized and integrated with structural measurements and lithological boundaries. Previous mappings by Jan and Mian (1971), Jan and Asif (1983) and Khalil and Afridi (1979) along the Ushu and Bhankhwarh rivers were field-verified and integrated. Western sections (Gabral–Shahibagh) were newly mapped during campaigns in 2023–2024. Digitization and georeferencing followed three main steps: high-resolution scanning, georeferencing in ArcMap using GeoTIFF topographic sheets (WGS84/UTM zone 43N), and digitizing lithological contacts and structures. The final map was vectorized using CorelDRAW.

## 5. Results

### 5.1. Field observations

The new geological map presents a significantly more detailed view of the study area's geology than previously available datasets. While the eastern section had been mapped by Jan and Mian (1971) and Jan and Asif (1983), the western part along the Gabral–Shahibagh rivers was previously unmapped. This study also includes new structural data, macroscopic lithological descriptions, and unit variations,

providing critical insights into the Cretaceous–Tertiary evolution of the central KA. To clarify the intrusion sequence, recent U–Pb zircon dating results were incorporated (Ahmad et al., 2025b). A detailed chronological description of the observed units follows.

### 5.1.1. The Kalam Group metasediments

The Kalam Group metasedimentary units in the Swat region of the central-western KA are interpreted as part of the Early Cretaceous Jaglot Group, as exposed in the eastern KA (Treloar et al., 1996). They occur in the southeastern part of the mapped area, generally trending northeast, though strike and dip vary, particularly in phyllites southwest of Kalam (Jan & Mian, 1971). The metasediments are intruded by the Late Cretaceous Matiltan Granite to the north, while their hornfelsic character to the south suggests intrusive contact with quartz diorite. Intrusive relationships are recorded by granitic dykes and metasediment xenoliths of in plutonic rocks (Jan & Mian, 1971).

The Kalam Group consists of low-grade (greenschist-facies) metamorphosed interbedded micaceous quartzites, phyllites, slates, and meta-limestones (Jan & Mian, 1971). At Shahu, the exposed quartzites, up to several kilometers thick, are folded into broad antiformal structures. The quartzites are foliated in the cm range, fine to very fine grained, and range in color from bluish gray on fresh surfaces to brown on weathered ones. The overlying phyllites exposed near Matiltan are a few hundred meter thick, more deformed, and medium to fine grained with light gray to brownish hues. Above these, slates (120–150 feet thick) are thin-bedded, fine grained, and red to green, often showing quartz and calcite veins. Overlying meta-limestones (~50 meter thick) are thin-bedded, foliated, and fossiliferous. Although the exact age of the Kalam Group is uncertain, the presence of Rhabdophyllian fauna fossils in the meta-limestone suggests a Mid-Jurassic to Early Cretaceous age (Bender & Raza, 1995).

### 5.1.2 Utror Volcanics

The Utror Volcanics form a prominent NE–SW trending belt in the west-central part of the Kohistan Arc (KA), occupying a large area in the southwestern part of the study area (Ushu Valley) and extend westward through northern Kalam, Utror, eastern and central Dir, and the Barawal Valley, reaching the Afghan border and beyond. The volcanics attain their maximum width (4–5 km) near Utror, while to the east, near Bhan, they are interbedded with slates and reach a thickness of approximately 3 km (Figure 2). Due to high elevation, extreme relief, and frequent landslides, the contacts between the volcanics and adjoining lithologies were often inaccessible. However, near Gabral, the volcanics are intruded by Late Paleocene quartz diorites, indicating intrusive contacts. To the southwest, the gently northwest-dipping volcanic units are bordered by metasedimentary rocks (quartzites and phyllites), which are stratigraphically situated beneath the volcanics (Jan & Mian, 1971). In the west, near Shahi, they occur interbedded with slates suggesting a temporal relationship between

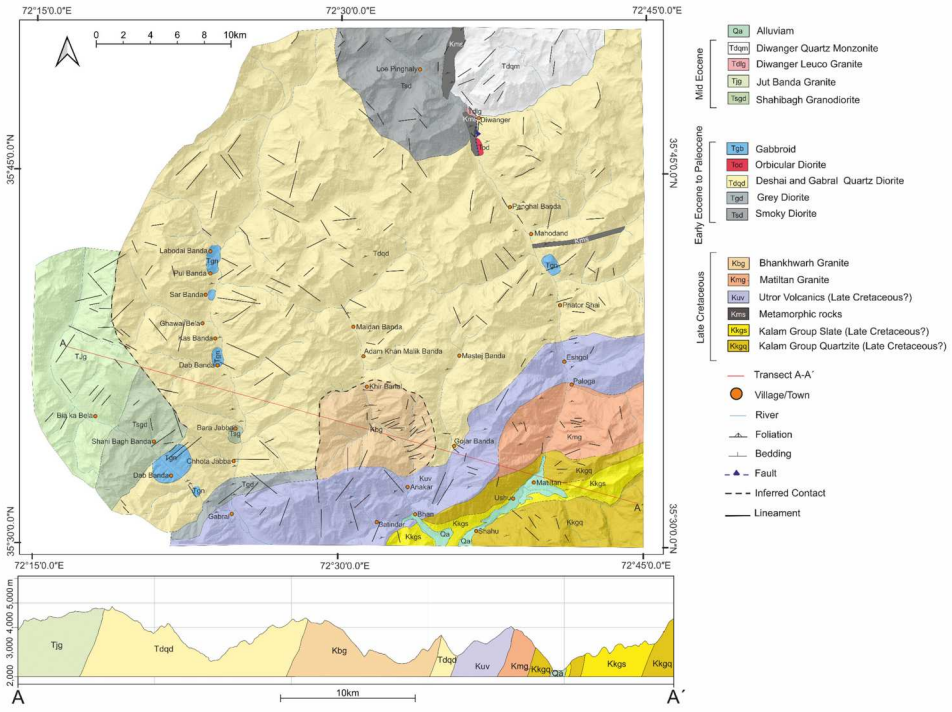


**Figure 2.** Geological map of the central Kohistan magmatic arc in northern Swat, Pakistan.

**Table. 1.** Sample locality, field, geochemical, and geochronological data for the studied representative samples.

| Sample ID | Geographic locality | Coordinates (dd) | Lithology | Field description / texture | Geochemical features | Age (U-Pb) |
|---|---|---|---|---|---|---|
| DU1 | Ushu | 35.53N, 72.68E | Phylite, slate | Medium- to fine-grained, thin-bedded, foliated | - | - |
| DU4 | Utror | 35.54N, 72, 56E | Rhyolite/dacite | Fine-grained to vitrophyric, foliated to non-foliated | Magnesian, peraluminous, calc-alkaline | - |
| MN43 | Matiltan | 35.59N, 72.68E | Granite | Medium- to coarse-grained, weakly foliated | Magnesian, peraluminous, high K-calc-alkaline | 77 ± 0.5 Ma |
| BK1 | Bhankhwarh | 35.55N, 72.56E | Granite | Coarse- to medium-grained, foliated | Magnesian, peraluminous, high K-calc-alkaline | 73 ± 0.5 Ma |
| LP3 | Loe Phingahley | 35.81N, 72.57E | Gabbroic Diorite | Medium-grained, massive | Magnesian, metaluminous, tholeiitic to calc-alkaline | 64 ± 0.5 Ma |
| GN5 | Gabral | 35.59N, 72.40E | Quartz Diorite | Medium- to coarse-grained, weakly to distinctly foliated | Magnesian, metaluminous, tholeiitic to calc-alkaline | 60 ± 0.4 Ma |
| MN1 | Deshai | 35.72N, 72.63E | Quartz Diorite | Coarse- to medium-grained, foliated to non-foliated | Magnesian, metaluminous, calc-alkaline | 53 ± 0.3 Ma |
| MN9 | Deshai | 35.76N, 72.61E | Orbicular diorite | Medium-grained, massive, orbicular | Magnesian, metaluminous, calc-alkaline | - |
| D3 | Diwanger | 35.78N, 72.61E | Quartz Monzonite | Porphyritic, massive | Magnesian, metaluminous, shoshonitic | 45 ± 0.4 Ma |
| GN15 | Shahibagh | 35.56N, 72.34E | Granodiorite | Coarse-grained, massive | Magnesian, metaluminous, high K-calc-alkaline | 46 ± 0.3 Ma |
| GN41 | Jut Banda | 35.60N, 72.27E | Granite | Porphyritic, massive | Magnesian, peraluminous, high K-calc-alkaline | 45 ± 0.3 Ma |
| MN27 | Mahodand | 35.88N, 72.66E | Gabbroid | Medium-grained, massive | Metaluminous, tholeiitic | - |
| GN8 | Gabral | 35.66N, 72.40E | Gabbroid | Medium-grained, massive | Metaluminous, calc-alkaline | - |
| GN13 | Shahibagh | 35.54N, 72.37E | Gabbroid | Medium-grained, massive | Metaluminous, tholeiitic | - |

the two units with eruption cycles alternating with sedimentation (Tahirkheli, 1979b).

The Utror Volcanics comprise andesitic and rhyolitic/dacitic rocks, predominantly occurring as volcaniclastic deposits, such as pyroclastic breccias., agglomerates, and tuffs, and subordinate lava flows (Table 1; Figure 3(a–f)). The volcanoclastic rocks predominate and are strongly sheared particularly around Bhan area (Figure 3(b)). The lava flow typically appear maroon or greenish, due to secondary alteration by hematite and epidote/chlorite, respectively. Rhyolitic/dacitic and andesitic lava flows are more common around Utror and Gabral. Rhyolitic flows exhibit bright gray colors, while andesitic ones are greenish gray – again reflecting the presence of secondary chlorite and epidote, indicative of a greenschist-facies overprint (Figure 3(c,d)). The lava flows generally show isotropic, fine-grained to vitrophyric textures and are often equigranular, although porphyritic varieties with feldspar phenocrysts (up to 1.5 cm) are also frequent in rhyolites (Figure 3(c)). Angular to rounded fragments up to 30 cm in diameter embedded in a tuffaceous or vitreous matrix (Figure 3(d)). Locally, cm-scale compositional banding results in variations in texture and color. Green andesitic rocks with spheroidal weathering textures are observed in some areas (Figure 3(e)), while pillow structures are rare. In places, cooling cracks within the volcanics are filled with carbonates (Figure 3(f)).

### 5.1.3. Matiltan granite

The Matiltan Pluton is a stock-sized granitic body covering approximately 10 km², located in the southeastern part of the mapped area (Table 1; Figures 2 and 4(a)). To the north and west, it is bordered by the Utror Volcanics, while to the south, it is in contact with metasedimentary rocks. The Matiltan Granite is generally weakly foliated, although more intensely foliated varieties are observed at specific localities, such as at 35°34′02″N, 72°40′18″E. The Matiltan Granite is bright gray in color, medium- to coarse-grained, and displays equigranular to sub-equigranular textures. Its mineralogical composition mainly includes quartz, plagioclase, alkali feldspar, with minor biotite and hornblende. Greenish streaks of epidote are frequently present, indicative of secondary alteration (Figure 4(b)). In some areas, the rock exhibits an overall greenish hue due to pervasive chloritization (Figure 4(c)). Small, dark-colored mafic enclaves (2–3 cm across) are occasionally observed. These enclaves are darker than the host granite and generally lack any clear internal foliation (Figure 4(b, c)).

### 5.1.4. Bhankhwarh granite

The Bhankhwarh pluton is a stock-sized granitic body located in the south-central part of the mapped area. It is bounded to the north by the Deshai Quartz Diorite and to the south by the Utror Volcanics (Table 1; Figures 2 and 4(d)). The nature of the contact between the Bhankhwarh Granite and the surrounding volcanics and quartz diorites remains unconfirmed due to the presence of extensive landslide deposits obscuring the contact zones. The granite ranges from weakly to distinctly foliated and is characterized by prominent jointing in three directions, which results in steep cliff faces. These joints also create a layered appearance from a distance (Figure 4(e)). The foliation trends northeast and dips moderately to the northwest. The

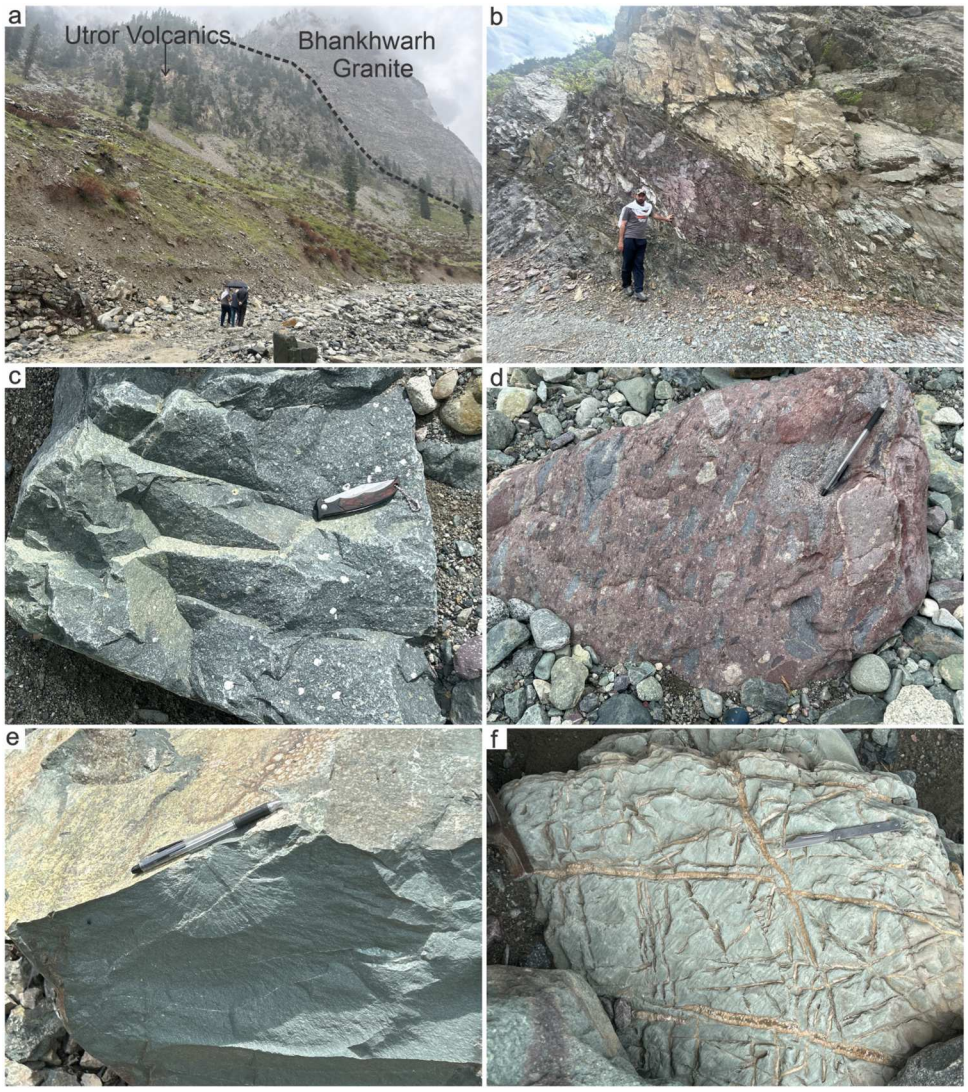


**Figure 3.** Field photographs of the Utror volcanics: (a) Outcrop view of contact between Utror Volcanics and Bhankhwarh granite; (b) 2.5 m thick zone of maroon volcanics bounded above by gray volcanics; (c) volcanic rock exhibiting porphyritic texture, having feldspar phenocryst with green color groundmass; (d) volcanic agglomerate containing abundant clasts of felsic volcanics of varying shape in pinkish volcanic matrix. Some of the enclaves are showing parallel stretching due to volcanic flow; (e) greenish gray (andesitic?) volcanics displaying spheroidal fractures and a felsic vein; (f) volcanic block showing anastomosing fracture-fillings of calcite.

granite is generally light in color, though parts of it exhibit a greenish hue due to chloritization (Figure 4(f)). Texturally, the granite is predominantly equigranular, though porphyritic varieties also occur. The latter feature tabular to lenticular plagioclase phenocrysts upto 5 mm set in a finer-grained, partly sheared groundmass composed of plagioclase, quartz, and minor biotite. Slickensided surfaces occasionally display secondary mineral assemblages of epidote, quartz, and white mica. Aplitic dykes, ranging from 3 to 7 cm in thickness, frequently crosscut the granite body (Figure 4(f)).

### 5.1.5. Smoky Diorite

The Smoky Diorite is mainly exposed northwest of the Diwanger confluence (Table 1; Figures 2 and 4(g)). To the northwest, it is separated from the Diwanger Monzogranite by a narrow zone of intercalated metamorphic rocks, granite, and diorite. To the south, it is bordered by banded amphibolites and extends westward toward the Doucher stream near Deshai, where it exhibits a sharp contact with the Deshai Quartz Diorite. The Smoky Diorite is dark gray, homogeneous, unfoliated, and medium- grained. It predominantly consists of equigranular plagioclase, hornblende, biotite, and minor pyroxene (Figure 4(h)). Locally, felsic pegmatite veins of variable thickness crosscut the diorite (Figure 4(i)), adding further textural and compositional complexity.

### 5.1.6. Gabral plutonites

Plutonic rocks of the Gabral Valley consist of gray diorites, quartz diorites, and hornblende-biotite gabbros. An alternation between light-colored quartz diorites and darker diorites and gabbros is frequently


**Figure 4.** Field photographs of the Matiltan granite (a–c), Bhankhwarh granite (d–f) and Smoky diorite (g–i). (a) Outcrop of Matiltan granite; (b) whitish foliated to weakly foliated granite hosting dark enclaves; bluish streaks probably due to chloritization; (c) bluish-green variety of Matiltan granite with color being due to chloritization; (d) outcrop of the contact between the Bhankhwarh granite and the Utror Volcanics; (e) outcrop of well-jointed Bhankhwarh granite; (f) light-colored weakly to distinctly foliated granite crosscut by aplitic veins up to 8 cm in width; (g) outcrop of Smoky diorite; (h) medium- to coarse-grained homogenous smoky diorite having reddish surface color due to weathering; (i) felsic vein of 20 cm width cross-cutting Smoky diorite.

observed. Locally, they are intruded by granitic bodies, as well as pegmatite and aplite veins.

*5.1.6.1. Gray diorite.* Gray diorite is exposed in the southwestern part of the mapped area, a few meters north of the northernmost outcrop of the Utror Volcanics near Gabral village (Figures 2 and 5(a)). Due to dense vegetation, the contact relationships between the gray diorite and the volcanics, as well as the Gabral quartz diorite, neighboring the gray diorite in the north, remain obscured. However, the presence of gray diorite xenoliths in the bordering Gabral quartz diorite suggests that the former represents an older intrusive phase. The gray diorite is weakly foliated, with the steeply dipping foliation trending NE–SW, and exhibits a medium- to fine-grained, equigranular texture. It is composed predominantly of plagioclase, hornblende, and biotite, with only minor quartz. The unit is devoid of xenoliths and is crosscut by whitish granitic dykes and felsic veins of varying thicknesses (Figure 5(a)).

*5.1.6.2. Gabral quartz diorite.* The weakly to distinctly foliated Gabral quartz diorite is exposed near Chotta Jabba in the southwestern part of the study area, approximately 1.5 km north of the Utror Volcanics and bordering the gray diorite (Table 1; Figures 2 and 5(b)). Further exposures occur northward along the Gabral River at Sario Jabba, Dab Banda, Kas Banda, Bailli Banda, Ghwai Bela, and Labodai Banda. While the quartz diorite in these localities shares a similar mineralogical composition, it exhibits variations in color (ranging from whitish to grayish) and fabric (from weakly foliated in the south to distinctly foliated in the north). The rock is medium- to coarse-grained and primarily composed of plagioclase, hornblende, and quartz (Figure 5(c)). It contains xenoliths of dark-gray diorite, varying in size and shape from 5 to 10 cm across (Figure 5(d)). These xenoliths occur In a variety of forms, including rounded, elongated, tabular, and lensoidal. The quartz diorite is locally intruded by mafic dykes up to 10 cm thick.

*5.1.6.3. Granites intrusions in the Gabral quartz diorite.* Granites occur as relatively small intrusions, up to 500 m in diameter, within the Gabral quartz diorite south of Bara Jabba in the southwestern part of the mapped area (Figure 2). These granites are very light in color, ranging from foliated to unfoliated, and exhibit a fine- to medium-grained, homogeneous texture. Mineralogically, they are composed predominantly of quartz, K-feldspar, and plagioclase, as well as minor biotite . Field relationships indicate that these granites intruded both the gray diorite and the Gabral quartz diorite.

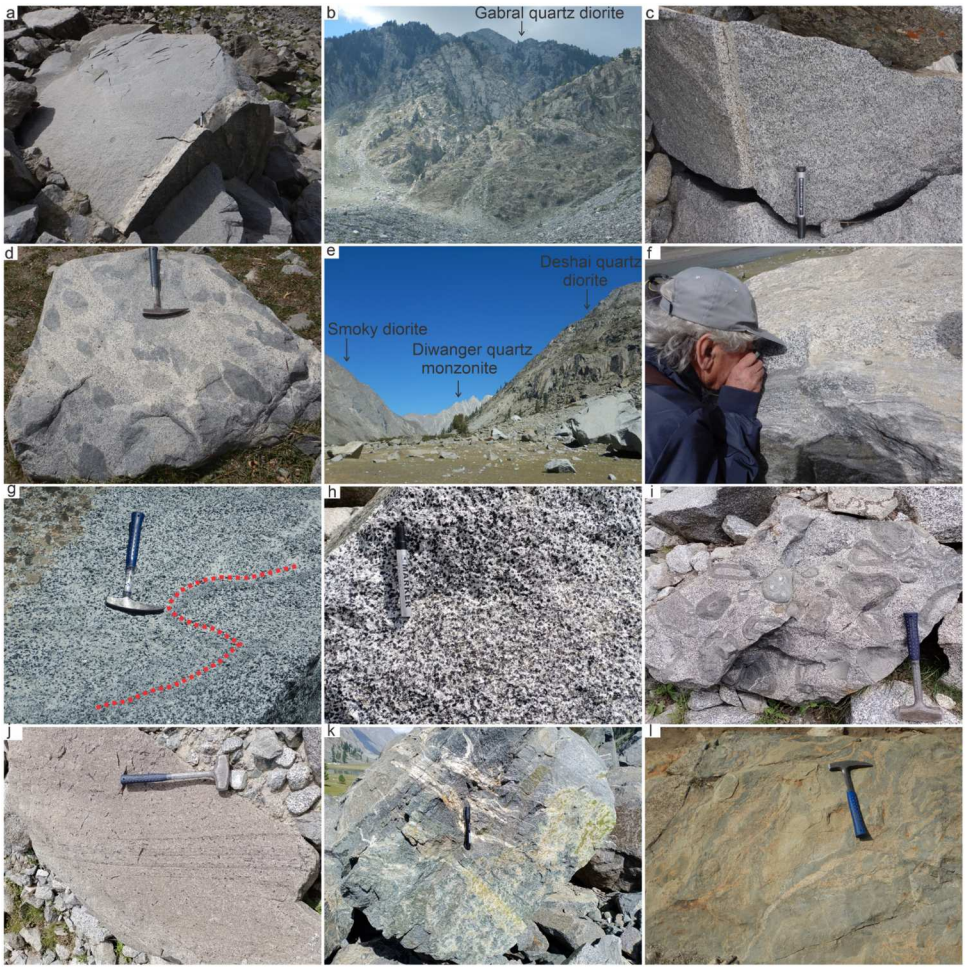


**Figure 5.** Field photographs showing (a) medium- to fine-grained gray diorite intruded by a 15 cm thick felsic vein; (b) outcrop view of Gabral quartz diorite; (c,d) light-colored, medium- to coarse-grained gneissose quartz diorite hosting abundant xenoliths of gray diorite; (e) outcrop view of Deshai quartz diorite, along with associated Smoky diorite and Diwanger quartz monzonite; (f) Deshai quartz diorite showing strong preferred orientation of light felsic and dark mafic minerals; (g) relatively coarser grained Deshai quartz diorite not having any preferred orientation which seems to be compositionally the same as gneissose diorite; (h) Deshai quartz diorite showing preferred orientation and S type folding; (i) orbicular diorite having rounded concentric orbicules; (j) brownish rock showing hornblende phenocryst and obvious layering; (k) banded country rock comprising strongly folded bands of dark to whitish color, and green color pistacite; (l) banded country rocks (migmatites?) with whitish leucosomes (white) and restite (dark) showing ptygmatic folding intruded by smoky diorite.

### *5.1.7. Deshai quartz diorite*

The Deshai quartz diorite constitutes the major plutonic unit in the mapped area. It extends from south of the Falak Sair Gol in the southeast to the Diwanger confluence in the north, and westwards to the Gabral–Shahibagh region (Table 1; Figures 2 and 5(e)). East of Diwanger, this unit likely continues toward the Dadarili Pass. Most exposures exhibit a well-developed gneissose fabric, characterized by aligned hornblende crystals trending NE–SW. In some locations, the rock is distinctly banded, displaying alternating layers rich in biotite-hornblende and plagioclase. The quartz diorites are transected by shear zones up to 2 cm wide, which are marked by a significant grain-size reduction (Figure 5(f, g)). The Deshai quartz diorite is coarse- to medium-grained, though finer-grained varieties also occur. It primarily consists of plagioclase, clinopyroxene, hornblende, quartz, Fe-oxides, and minor biotite. A non-foliated, coarse-grained variety hosting large hornblende and biotite crystals is more common in the northern part of the Ushu River section and is interpreted as a local facies of the Deshai pluton (Figure 5(h)). Coarse-grained blocks can reach several meters in diameter, while medium-grained blocks are typically <2 m across. Some quartz diorites appear darker due to higher mafic mineral content, yet they still display a distinct foliation. South of the Falak Sair River, the Deshai quartz diorite shows significant compositional heterogeneity, with local intrusions of quartz monzonite, granite, and dark diorite.

Near Deshai, the diorites exhibit striking orbicular textures (at Table 1; Figure 4(i)). Due to steep topography and extensive land-sliding, the precise spatial relationship between these orbicular diorites and the surrounding Deshai quartz diorite remains uncertain. The orbicules occur sporadically, embedded within a medium-grained diorite matrix. According to Symes

et al. (1987), the orbicules consist of concentric shells of clinopyroxene, orthopyroxene, hornblende, and plagioclase encasing a central, highly recrystallized dioritic core. A dioritic boulder at 35°46′04″N, 72° 36′54″E exhibits cm-scale layering of hornblende and plagioclase (Figure 5(j)).

Approximately 1 km south of Mahodand Lake, a c. 300 m wide, steeply dipping and NE–SW trending heterogeneous zone is exposed (Figure 2), which consists of dark, foliated to unfoliated Deshai quartz diorite interlayered with a strongly folded and banded diorite, characterized by boudinaged whitish, mm- to cm-thick plagioclase-rich bands alternating with hornblende-rich layers (Figure 5(k)). Epidote-rich veins are observed along fracture planes (Figure 5(k)).To the northwest of the Diwanger confluence, a major exposure of these interlayered lithologies spans approximately 2 km in length and 0.5 km in width. The rocks exhibit rhythmic banding of alternating plagioclase-rich (whitish) and hornblende-rich (dark) layers that show conspicuous ptygmatic folding and micro-folding (Figure 5(l)). They are fine- to medium-grained and composed mainly of plagioclase and hornblende, with minor occurrences of pyroxene. Concordant veins of porphyritic granite and Smoky diorite, ranging from 1 to 5 cm in width, locally transect the folded rocks.

Locally, narrow mafic dykes and veins, typically less than 30 cm wide, intrude the Deshai quartz diorite (Figure 6(a)). They exhibit sharp contacts with the Deshai quartz diorite and rarely crosscut the penetrative foliation of the host. These dykes are dark green, fine- to medium-grained, equigranular, and primarily composed of plagioclase, hornblende, and biotite. Some display a weak flow banding parallel to the dyke walls. Near Mahodand, a 10-meter-sized boulder of micro-diorite is cut by numerous quartzo-feldspathic veins (Figure 6(b)). The Deshai quartz diorite also contains rare pegmatite dykes (quartz-feldspar-hornblende-tourmaline pegmatite), aplitic dykes and quartz-feldspar veins (Figure 6(c, d)). Some of these dykes are foliated, indicating emplacement prior to the development of the host rock's gneissose fabric (Figure 6(d)). North of Diwanger, abundant hornblende-rich patches and veins occur in the Deshai quartz diorite, locally forming dense vein networks. These features may reflect infiltration of the Deshai quartz diorite by younger magmas or fluids. The Deshai quartz diorite also hosts rare pegmatite dykes, composed of quartz, feldspar, hornblende, and tourmaline, as well as aplitic dykes and quartz-feldspar pegmatites.

Randomly distributed mafic xenoliths and microgranular enclaves are present within the Deshai quartz diorite, with their abundance decreasing from south to north. The xenoliths vary in size (3–12 cm), shape (elliptical, rounded to subrounded, angular to subangular, and elongated), and color (melanocratic to mesocratic) (Figure 6(e–h)). The contact of microgranular enclave with the host quartz diorite ranges from sharp to diffuse, lobate, or embayed (Figure 6(f)). Moderately to highly stretched mesocratic enclaves often appear subrounded to ellipsoidal. Some enclaves feature thin, fine-grained margins and show signs of impregnation by the host quartz diorite (Figure 6(g)). In gneissose host rocks, the enclaves are aligned parallel to the foliation (Figure 6(h)). They are fine-grained, exhibit massive textures, and resemble the host rock macroscopically, apart from their darker color, which reflects a higher modal content of mafic minerals and smaller grain size.

### 5.1.8. Gabbroic plugs

*5.1.8.1. Mahodand hornblende gabbro.* Approximately one kilometer north of the Falakser River, a dark hornblende gabbro dyke, c. 1.5 km in length, intrudes the Deshai quartz diorite (Table 1; Figures 2 and 7(a)). The gabbro is dark greenish in color, medium-grained, and exhibits a massive, homogeneous texture. It is primarily composed of pyroxene, hornblende, and plagioclase (Figure 7(b–d)). It contains dark mafic cumulus phases of up to 30 cm across, composed of hornblende, plagioclase, and minor biotite, with grain sizes generally less than 2 cm (Figure 7(c)). Notably, the hornblende crystals frequently contain abundant inclusions of plagioclase. The hornblende gabbro hosts mafic veins, typically 2–4 cm thick, which are predominantly composed of hornblende with minor plagioclase. The plagioclase grains in these veins may reach lengths of up to 1 cm and are locally rimmed by hornblende (Figure 7(d)). Chlorite is commonly observed along fractures, suggesting its late-stage hydrothermal formation.

*5.1.8.2. Gabral diorite and gabbronorite.* The second most abundant rock unit in the Gabral Valley comprises are gabbroids (Table 1; Figure 2). These rocks exhibit sharp intrusive contacts with the Gabral quartz diorite and occur periodically as 1–1.5 km thick plugs or dykes (Figure 7(e)). These diorites are exposed in the vicinity of Bara Jabba, Dab Banda, Sar Banda, and Labodai Banda areas. They consist of plagioclase, hornblende, biotite, ± pyroxene, and Fe–Ti oxides. Based on the presence or absence of pyroxenes, they are further subdivided into hornblende-biotite diorite and hornblende-biotite gabbronorite. Both lithologies are homogeneous, medium- to coarse-grained, and massive, lacking any prominent jointing or fracturing. Locally, they are intruded by fine-grained mafic dykes up to 5 cm in thickness (Figure 7(f)). While xenoliths are absent, sparse gray-colored autoliths of similar mineralogical composition are occasionally observed.

*5.1.8.3. Shahi Bagh gabbronorite.* Small, dark-colored gabbronorite bodies occur as plugs and dykes within

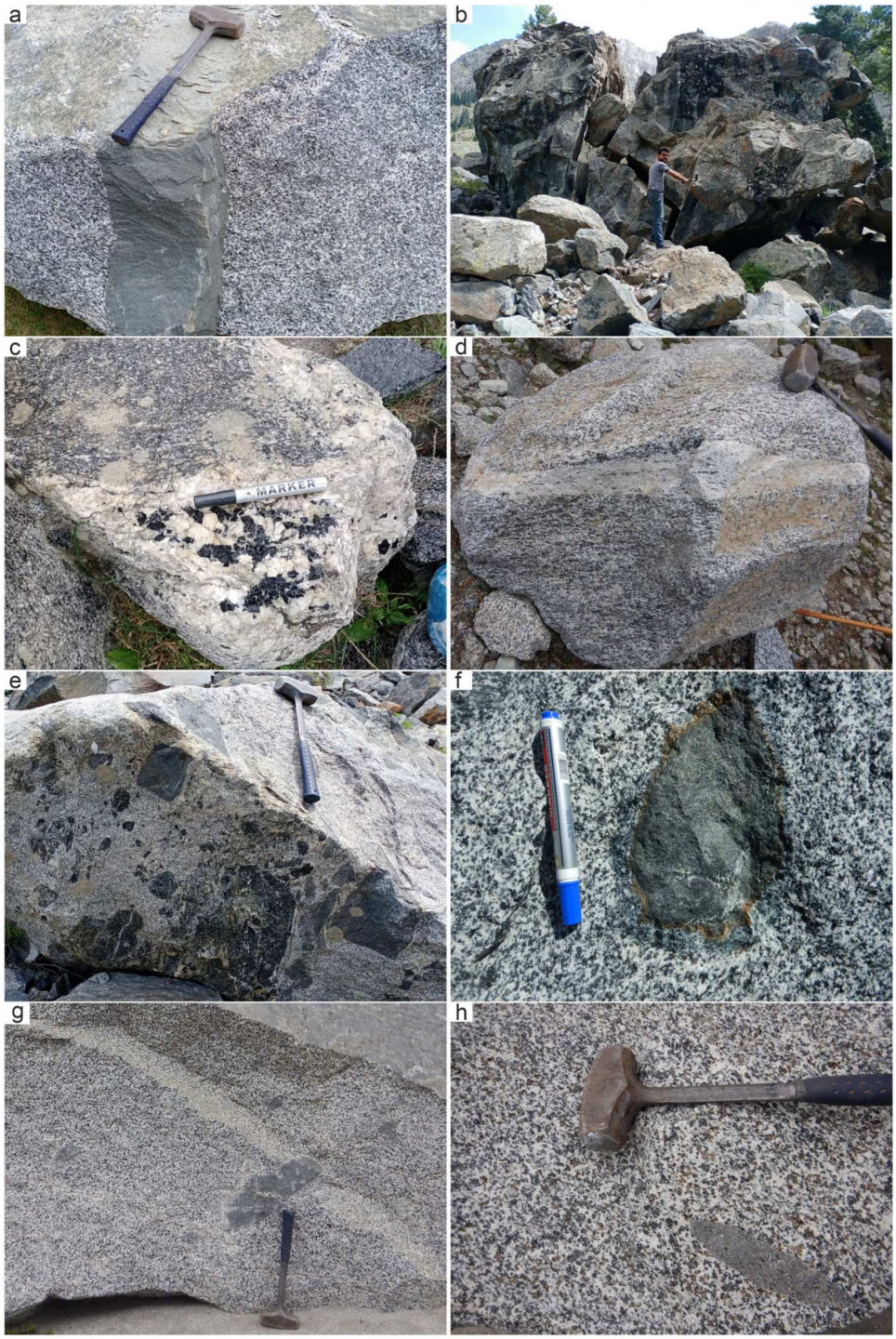


**Figure 6.** Field photographs of dykes and veins within Deshai quartz diorites (a) A 20 cm thick mafic dyke; (b) ten meter-sized boulder of micro-diorite having numerous quartzo-feldsphatic veins; (c) Quartz-feldspar-hornblende-tourmaline pegmatite; (d) deformed aplitic dykes and quartz-feldspar veins, 20 cm in width, in Deshai quartz diorite, (e) gneissose quartz diorite hosting mafic enclaves. The white part looks like a leucogranite with stretched enclaves and folded bands ; (f) fine- grained mafic enclave showing a diffuse boundary with host quartz diorite; (g) impregnated enclave in quartz diorite; (h) elongated enclave orientated parallel to the foliation direction of quartz diorite.

quartz diorite near Yakh Banda, located in the south-western part of the mapped area (Table 1; Figure 2). These intrusions are equigranular, medium- to coarse-grained, and homogeneous in texture, and they are notably devoid of xenoliths (Figure 7(g, h)). The gabbronorites are characterized by the frequent presence of rectangular purple pyroxene crystals, accompanied by plagioclase and hornblende. Greenish chlorite is observed on some joint surfaces, likely representing secondary alteration. Locally, these rocks are intruded by dark hornblende-biotite-rich pegmatitic veins, which contain hornblende crystals up to 12 cm in length (Figure 7(g)). Additionally, a felsic vein up to 40 cm wide is present at one locality, distinguished by the abundance of hornblende and plagioclase crystals measuring up to 3 cm in length (Figure 7(h)). In

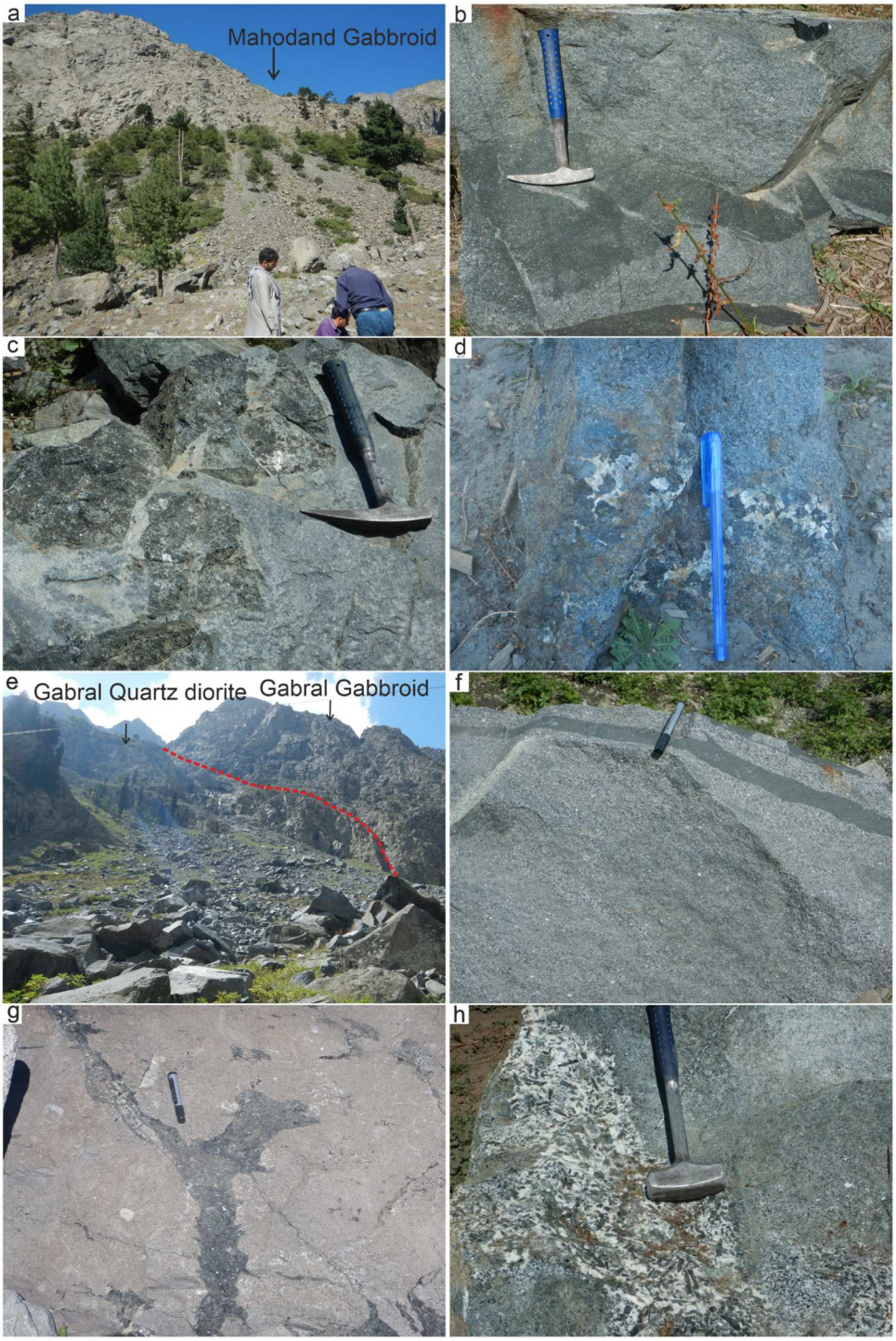


**Figure 7.** (a) Outcrop view of gabbroid plug within the Deshai quartz diorite; (b) gabbroic rock with the center zone being very dark, the other (more abundant) being gray and showing intrusive relationship with the dark zone; (c) 4 to 8 cm thick ultramafic cumulus phase possibly full of hornblende and plagioclase, surrounded by gray matrix; (d) 4 cm thick mafic veins full of hornblende crystals of up to 1 cm in length. Exposed surface contains euhedral hornblende of up to 1 cm in length and subrounded plagioclase grains of up to 1 cm which are surrounded by black rims; (e) dark gabbronorite plug within Gabral quartz diorite; (f) dark-colored medium-grained, homogenous, massive gabbronorite intruded by 5 cm mafic dyke; (g) equigranular diorite/gabbro intruded by hornblende pegmatite vein having thickness of 3–5 cm; (h) gabbroid intruded by hornblende-rich felsic vein having thickness of 30 cm.

certain areas, surface exposures of the gabbronorite exhibit a whitish color attributed to weathering.

### *5.1.9. Diwanger quartz monzonite*

Steep cliffs of the Diwanger quartz monzonite in the Mahodand valley are already visible from several kilometers away (Table 1; Figures 2 and 8(a)). This unit represents one of the youngest intrusive bodies in the mapped area. It forms a stock-sized pluton, previously referred to as the 'Diwanger granite' by Jan and Mian (1971). The quartz monzonite stock extends northeastward up to the Dadarili Pass. To the west, it

intrudes a narrow belt of metamorphic rocks that separates it from the Smoky diorite. The quartz monzonite exhibits sharp intrusive contacts with both the older Deshai quartz diorite and the Smoky diorite. The deeply incised, northeast-trending eastern flank of the Diwanger confluence marks the boundary between the Diwanger quartz monzonite and the Deshai quartz diorite. The Diwanger quartz monzonite is well-jointed, and its tendency to break along these joints contributes to the development of steep cliffs characteristic of this unit. It is homogeneous, whitish-gray, generally non-foliated, coarse-grained, and porphyritic, with plagioclase phenocrysts reaching up to 5 cm in length (Figure 8(b)). It is primarily composed of plagioclase, K-feldspar, and quartz, with accessory hornblende and biotite. Dark diorite xenoliths are present within the quartz monzonite. Locally, pegmatite veins of variable thickness crosscut the quartz monzonite. A small associated body of medium-grained, non-porphyritic granite is also present (Figure 8(c)). According to Jan and Mian (1971), this granite resembles the matrix of the surrounding porphyritic quartz monzonite. It has been suggested that, during the intrusion of thin dykes, the phenocrysts were too large to be transported by the melt, resulting in this distinct non-porphyritic phase.

#### 5.1.10. Sahi Bagh granitoids

The Shahi Bagh valley in the eastern study area contains a heterogeneous suite of rocks, including gray diorite, quartz diorite, hornblende gabbronorite, Shahibagh granodiorite, Jut Banda granite, tourmaline-bearing gray granite, leucogranite, and aplite (Figure 2). About 2 km east of Gabral, gray diorite predominates, bordered to the northwest by light-colored quartz diorite, followed by gabbronorite, granodiorite, and granite bodies. Detailed descriptions of gray


**Figure 8.** Field photographs showing (a) towering cliffs of Diwanger Quartz monzonite, Smoky diorite, and Deshai quartz diorite; (b) light- colored porphyritic Diwanger quartz monzonite with feldspar phenocrysts of up to 5 cm in length; (c) medium- to coarse-grained non-porphyritic Diwanger Leucogranite associated with Diwanger quartz monzonite; (d) Outcrop of Shahibagh granodiorite; (e) Shahibagh granodiorite hosting abundant enclaves of varying shapes and sizes. At least some of the elongated enclaves show parallel arrangement; (f, g) medium- to course-grained Shahibagh granodiorite intruded by pegmatitic veins containing pink K-feldspar, plagioclase, quartz, white mica, and black tourmaline; (h) coarse-grained porphyritic Jut Banda granite with pinkish K-feldspar phenocrysts and hosting an eye-shaped mafic enclave; (i) Jut Banda granite having fractures filled with greenish copper ore ; (j) Jut Banda granite containing xenolith of gray granite; (k) tourmaline bearing gray granite hosting rounded tourmaline-rich enclaves with white reaction rims; (l) medium-grained massive leucogranite associated with the Jut Banda granite.

diorite, quartz diorite, and gabbronorite are given earlier, with granodiorites and granites described below.

*5.1.10.1. Shahi Bagh granodiorites.* The Shahi Bagh granodiorite, exposed north of the Shahi Bagh gabbronorite and extending 4 km to Biah, is coarse-grained, slightly porphyritic, and mostly unfoliated, with local foliation (Table 1; Figures 2 and 8(e–g)). It mainly consists of plagioclase, quartz, orthoclase, biotite, and hornblende. Mafic enclaves with sharp boundaries, subrounded to elliptical and 12–16 cm long, increase in size and abundance toward the northern pluton boundary (Figure 8(e)). Locally, the granodiorite shows orbicular textures with sub-circular to ellipsoidal orbicules of 8–12 cm diameter in diameter, featuring dark mafic cores and less mafic shells with diffuse margins. Pegmatitic veins up to 30 cm thick intrude the granodiorite, containing pink K-feldspar phenocrysts (3–4 cm), plagioclase, quartz, white mica (2–3 cm), and tourmaline (up to 1.5 cm) (Figure 8(g)).

*5.1.10.2. Jut Banda granite.* The Jut Banda granite, north of the Shahi Bagh granodiorite, is massive, light-colored, coarse-grained, and porphyritic with pink K-feldspar phenocrysts (Table 1; Figure 8(h–j)). It is mainly exposed as fresh, unjointed blocks and locally contains eye-shaped dark enclaves up to 16 cm long (Figure 8(h)). Thin chalcopyrite veins up to 2 mm wide are present (Figure 8(i)). The granite locally hosts xenoliths of gray granite (Figure 8(j)).

*5.1.10.3. Tourmaline-bearing grey granite.* Another granite variety in the Shahi Bagh valley, associated with the Jut Banda granite, is a medium-grained, homogeneous, equigranular granite featuring undeformed, rounded tourmaline-rich enclaves surrounded by felsic shells (Figure 8(k)). It is light gray and composed of quartz, plagioclase, K-feldspar, and minor biotite. Locally, whitish leucocratic granite varieties lacking visible mafic minerals also occur (Figure 8(l)).

### 5.2. Structures

Metasediments of the Kalam Group, i.e. the oldest rock unit exposed in the mapped area, show a strong NE–SW foliation, with predominantly steep dips (70–80°) toward northwest (Table S1). Kalam metasediments exhibit Dome-like folding which likely results from intrusion of the granitoid plutons. The volcanic belt of the Utror volcanics also trends NE–SW, with main dips of 60 to 78° directed to northwest, however local variability is present due to volcanic layering and proximity to intrusive contact (Table S1).

The Bhankhwarh and Matiltan granite and the Deshai and Gabral quartz diorites show strong planar fabrics defined by aligned plagioclase, biotite, and hornblende, crystals showing foliations strike NE–SW (Table S1). The dip angles, however, show slight variation between plutons with Bhankhwarh granite dips 75–80° toward the northwest, Matiltan granite 75–82° NW, and the Deshai-Gabral Quartz Diorites dips 60–85° NW (Table S1). The intensity of foliation increases southward toward the volcanic contacts but weakens or even disappears to the NE and NW. Accordingly, these structures likely reflect pluton emplacement along active shear zones with a minor tectonic overprint during or after solidification. Well-developed joints, especially in Bhankhwarh granite, dip northwest.

South of the Diwanger confluence, a lithological shift from banded diorite (west bank) to quartz diorite (east bank) along the Ushu River suggests presence of a sinistral fault, offsetting western units southward relative to the east, as already noted by Jan and Mian (1971) (Figure 2). Notably, most deeply incised valleys align with rock contacts, except the Ushu River, which apparently follows this major sinistral strike-slip fault.

## 6. Discussion and conclusions

The new geological map offers the yet most detailed presentation of northern Swat Kohistan's geology, identifying the following lithologies (from oldest to youngest): Cretaceous Kalam Group metasediments, Late Cretaceous Utror volcanics, Matiltan and Bhankhwarh granites, Paleocene-Early Eocene Smoky diorites, Gabral-Deshai quartz diorites, and gabbroic rocks, and Mid-Eocene granitoids (Diwanger quartz monzonites, Shahi Bagh granodiorite, Jut Banda granite).

Cretaceous metasediments in the south, i.e. turbidites from an extensional back- or intra-arc basin (Treloar et al., 1996), are overlain by Utror volcanics and intruded by Late Cretaceous–Paleocene granites and diorites, suggesting the metasediments acted as country rocks. The oldest magmatism in the central-western KA is Late Cretaceous (77–73 Ma). These granitoids are relatively quartz-rich, with variable mineralogy, reflecting different emplacement histories. Notably, the Bhankhwarh granite is more fractionated than the Matiltan granite. Formation of chlorite and epidote reflect late-stage hydrothermal alteration. A local foliation along the pluton boundaries indicates syn-emplacement shearing.

Paleocene to Early Eocene Smoky diorite, gray diorite, and Deshai-Gabral quartz diorite are more mafic in composition. Gray diorite xenoliths in the Deshai quartz diorite indicate that the former is older. Formation of Gabral-Deshai quartz diorite occurred at c. 53 Ma. Banded quartz diorites in the northern part of the study area show a gneissic fabric with micro-folds and boudinage, indicating ductile deformation along local shear zones. The dioritic plutons are crosscut by mafic and felsic dykes and late-

stage epidote-bearing hydrothermal veins. Gabbro bodies intrude the quartz diorites as plugs and dykes, marked by sharp contacts, suggesting a later, likely post-collisional intrusive event. Younger Mid-Eocene granitoids (Shahibagh granodiorite and Diwanger and Jut Banda granites) intrude the Deshai-Gabral quartz diorites. Tourmaline-bearing granites and leucogranites represent strongly fractionated, late-stage magmas.

## Software

For georeferencing the documents and the elaboration of the final digitized cartography ArcMap 10.8.2 software was used. The geological map was improved by editing the vector file with CorelDRAW 2021 software.

## Acknowledgments

Thanks to my colleagues Abuzar Ghaffari, Umair Mussawer, and Adeel from NCEG for field assistance, and Luqman Hussain (NCEG) for GIS support. We gratefully acknowledge the support of the editor-in-chief, Dr. Mike Smith, and the associate editor, Dr. Jasper Knight, as well as three reviewers, Huan Li, Santosh Kumar and Makram Murad-al-Shaikh, for constructive suggestions that helped to improve the manuscript.

## Disclosure statement

No potential conflict of interest was reported by the author(s).

## Funding

This work was supported by the Deutsche Forschungsgemeinschaft (DR 744/10-1). Financial support from the Higher Education Commission (HEC) of Pakistan and Deutscher Akademischer Austauschdienst (DAAD) is gratefully acknowledged. The Graduate School for Climate and Environment (GRACE), KIT, and the National Centre of Excellence in Geology (NCEG), University of Peshawar, funded geological field trips. M. Q. Jan acknowledges grants from the Pakistan Academy of Sciences (PAS RG103) and the Chinese Academy of Sciences (PIFI) for research in northern Pakistan.

## Data availability statement

The authors confirm that the data supporting the findings of this study are freely available within the article.

## References

Ahmad, T., Arif, M., Qasim, M., & Sajid, M. (2021a). Petrology of granitoids from Indus syntaxis, northern Pakistan: Implications for paleo-proterozoic A-type magmatism in north-western Indian plate. *Geochemistry*, *81*(1), 1–21. https://doi.org/10.1016/j.chemer.2020.125693

Ahmad, T., Drüppel, K., Jan M, Q., Zeh, A., & Gerdes, A. (2025b). Tectono-magmatic evolution of the central Kohistan magmatic arc, Pakistan – new constraints from zircon U-Pb dating, Hf isotopes and geochemistry. *Journal of Petrology*.

Ahmad, T., Rizwan, M., Hussain, Z., Ullah, S., Ali, Z., Khan, A., … Khan, H. A. (2021b). Mineralogical and textural influence on physico-mechanical properties of selected granitoids from Besham syntaxis, northern Pakistan. *Acta Geodynamica et Geomaterialia*, *18*(3), 347–362. https://doi.org/10.1316/8AGG.2021.0024

Bard, J. P. (1983). Metamorphism of an obducted island arc: Example of the Kohistan sequence (Pakistan) in the Himalayan collided range. *Earth and Planetary Science Letters*, *65*(1), 133–144. https://doi.org/10.1016/0012-821X(83)90195-4

Bender, F. K., & Raza, H. A. (1995). "*Geology of Pakistan*" *borntraeger*. Stuttgart.

Bouilhol, P., Jagoutz, O., Hanchar, J. M., & Dudas, F. O. (2013). Dating the India-Eurasia collision through arc magmatic records. *Earth and Planetary Science Letters*, *366*, 163–175. https://doi.org/10.1016/j.epsl.2013.01.023

Burg, J. P. (2011). The Asia-Kohistan-India collision: Review and discussion. *Frontiers in Earth Sciences*, *4*, 279–309. https://doi.org/10.1007/978-3-540-88558-0_10

Dhuime, B., Bosch, D., Garrido, C. J., Bodinier, J. L., Bruguier, O., Hussain, S. S., & Dawood, H. (2009). Geochemical architecture of the lower- to middle-crustal section of a paleo-island arc (Kohistan complex, Jijal-Kamila area, northern Pakistan): implications for the evolution of an oceanic subduction zone. *Journal of Petrology*, *50*(3), 531–569. https://doi.org/10.1093/petrology/egp010

Gaetani, M. (1997). The Karakorum Block in Central Asia, from ordovician to cretaceous. *Sedimentary Geology*, *109*(3–4), 339–359. https://doi.org/10.1016/S0037-0738(96)00068-1

Heuberger, S., Schaltegger, U., Burg, J. P., Villa, I. M., Frank, M., Dawood, H., Hussain, S., & Zanchi, A. (2007). Age and isotopic constraints on magmatism along the Karakoram-Kohistan suture zone, NW Pakistan: Evidence for subduction and continued convergence after India-Asia collision. *Swiss Journal of Geosciences*, *100*(1), 85–107. https://doi.org/10.1007/s00015-007-1203-7

Ivanac, J. F., Traves, D. M., & King, D. (1956). The geology of the north- west portion of Gilgit agency, Pakistan. *Geological Survey of Pakistan*, *8*(2), 1–27.

Jagoutz, O., Bouilhol, P., Schaltegger, U. R. S., & Müntener, O. (2018). The isotopic evolution of the Kohistan Ladakh arc from subduction initiation to continent arc collision. *Geological Society, London, Special Publication*, *483*(1), 165–182. https://doi.org/10.1144/SP483.7

Jagoutz, O., Muntener, O., Burg, J., Ulmer, P., & Jagoutz, E. (2006). Lower continental crust formation through focused flow in km-scale melt conduits: The zoned ultramafic bodies of the Chilas complex in the Kohistan Island arc (NW Pakistan). *Earth and Planetary Science Letters*, *242*(3–4), 320–342. https://doi.org/10.1016/j.epsl.2005.12.005

Jagoutz, O., & Schmidt, M. W. (2012). The formation and bulk composition of modern juvenile continental crust: The Kohistan arc. *Chemical Geology*, *298–299*, 79–96. https://doi.org/10.1016/j.chemgeo.2011.10.022

Jan, M. Q. (1979a). Petrography of pyroxene granulites from northern Swat and Kohistan. *Journal of Himalayan Earth Sciences*, *11*(1), 65–87.

Jan, M. Q. (1979b). Petrography of the amphibolites of Swat and Kohistan. *Journal of Himalayan Earth Sciences*, *11*(1), 51–64.

Jan, M. Q. (1988). Geochemistry of amphibolites from the southern part of the Kohistan arc, N. Pakistan. *Mineralogical Magazine*, *52*(365), 147–159. https://doi.org/10.1180/minmag.1988.052.365.02

Jan, M. Q., & Asif, M. (1983). Geochemistry of tonalites and (quartz) diorites of the Kohistan-Ladakh (Transhimalyan) granitic belt in Swat, NW Pakistan. In F. A. Shams (Ed.), *Granites of himalaya, Karakoram and Hindukush* (pp. 355–376).

Jan, M. Q., Asif, M., Tahirkheli, T., & Kamal, M. (1981). Tectonic subdivision of granitic rocks of northern Pakistan. *Journal of Himalayan Earth Sciences*, *14*(1), 159–182

Jan, M. Q., & Howie, R. A. (1981). The mineralogy and geochemistry of the metamorphosed basic and ultrabasic rocks of the Jijal complex, Kohistan, NW Pakistan. *Journal of Petrology*, *22*(1), 85–126. https://doi.org/10.1093/petrology/22.1.85

Jan, M. Q., Khan, M. A., & Qazi, M. S. (1993). The Sapat Mafic-ultramafic complex, Kohistan Arc, north Pakistan. *Geological Society, London, Special Publications*, *74*(1), 113–121. https://doi.org/10.1144/GSL.SP.1993.074.01.09

Jan, M. Q., & Mian, I. (1971). Preliminary geology and petrography of Swat Kohistan. *Journal of Himalayan Earth Sciences*, *1*(6), 1–32.

Jan, M. Q., Ullah, R., & Anjum, M. N. (2025). Magmatic (Cr–Ni–PGE) and secondary/hydrothermal (Emerald–Peridot–Rodingite–Nephrite jade) mineralization associated with ultramafic–mafic complexes of Pakistan. *Geological Society, London, Special Publications*, *552*(1), 1–48. https://doi.org/10.1144/SP552-2023-99

Kazmi, A. H., & Jan, M. Q. (1997). *Geology & tectonics of Pakistan*. Graphic Publisher. p. 554.

Kempe, D. R., & Jan, M. Q. (1970). An alkaline igneous province in the north-west frontier province, west Pakistan. *Geological Magazine*, *107*(4), 395–398. doi:10.1017/S0016756800056260

Khalil, M., & Afridi, A, G, K. (1979). "The geology and petrography of Deshai-Diwangar Area; Ushu Gol Valley, Swat Kohistan. *Journal of Himalayan Earth Sciences*, *11*(1), 99–111.

Khan, A., Ullah, Z., Li, H., Faisal, S., & Rahim, Y. (2025). Apatite texture, trace elements and Sr-Nd isotope geochemistry of the Koga carbonatite-alkaline complex, NW Pakistan: Implications for petrogenesis and mantle source. *Chemical Geology*, *676*, 122611. https://doi.org/10.1016/j.chemgeo.2025.122611

Khan, M. A., Jan, M. Q., & Weaver, B. L. (1993). Evolution of the lower arc crust in Kohistan, N. Pakistan: Temporal arc magmatism through early, mature and intra-arc rift stages. *Geological Society, London, Special Publications*, *74*(1), 123–138. https://doi.org/10.1144/GSL.SP.1993.074.01.10

Khan, M. A., Jan, M. Q., Windley, B. F., Tarney, J., & Thirlwall, M. F. (1989). The Chilas Mafic-ultramafic igneous complex; the root of the Kohistan Island Arc in the Himalaya of northern Pakistan. In L. L. Malinconico & R. J. Lillie (Eds.), *Tectonics of the western Himalayas* (pp. 75–94). Geological Society of America, Special Papers. https://doi.org/10.1130/SPE232-p75.

Khan, T., Jan, M. Q., Khan, M. A., & Kausar, A. B. (1997). High-grade metasedimentary rocks (Gilgit formation) in the vicinity of Gilgit, Kohistan, northern Pakistan. *Journal of Mineralogy, Petrology and Economic Geology*, *92*(11), 465–479. https://doi.org/10.2465/ganko.92.465

Martin, C. R., Jagoutz, O., Upadhyay, R., Royden, L. H., Eddy, M. P., Bailey, E., Nichols, C. I. O., & Weiss, B. P. (2020). Paleocene latitude of the Kohistan–Ladakh Arc indicates multistage India–Eurasia collision. *Proceedings of the National Academy of Sciences*, *117*(47), 29487–29494. doi:10.1073/pnas.2009039117

Petterson, M. G. (2010). A review of the geology and tectonics of the Kohistan Island Arc, north Pakistan. *Geological Society, London, Special Publication*, *338*(1), 287–327. https://doi.org/10.1144/SP338.14

Petterson, M. G., & Windley, B. F. (1985). Rb-Sr dating of the Kohistan arc-batholith in the trans-Himalaya of north Pakistan, and tectonic implications. *Earth and Planetary Science Letters*, *74*(1), 45–57. doi:10.1016/0012-821X(85)90165-7

Petterson, M. G., & Windley, B. F. (1991). Changing source regions of magmas and crustal growth in the trans-Himalayas-evidence from the Chalt Volcanics and Kohistan Batholith, Kohistan, northern Pakistan. *Earth and Planetary Science Letters*, *102*(3-4), 326–341. doi:10.1016/0012-821X(91)90027-F

Pudsey, C. J. (1986). The northern suture, Pakistan: Margin of a cretaceous island arc. *Geological Magazine*, *123*(4), 405–423. https://doi.org/10.1017/S0016756800033501

Searle, M. P. (2011). Geological evolution of the Karakoram ranges. *Italian Journal of Geosciences*, *130*(2), 147–159. https://doi.org/10.3301/IJG.2011.08

Searle, M. P., Khan, M. A., Fraser, J. E., Gough, S. J., & Jan, M. Q. (1999). The tectonic evolution of the Kohistan-Karakoram collision belt along the Karakoram highway transect, north Pakistan. *Tectonics*, *18*(6), 929–949. https://doi.org/10.1029/1999TC900042

Tahirkheli, R. A. K. (1979). Geology of Kohistan and adjoining Eurasian and indo-Pakistan continents, Pakistan. *Geological Bulletin of University of Peshawar*, *1*(11), 1–30.

Tahirkheli, R. A. K., & Jan, M. Q. (1979). Geology of Kohistan, Karakoram, Himalaya, northern Pakistan. *Geological Bulletin of University of Peshawar*, *1*(11), 1–187.

Treloar, P. J., Brodie, K. H., Coward, M. P., Jan, M. Q., Khan, M. A., Knipe, R. J., Rex, D. C., & Williams, M. P. (1990). The evolution of the Kamila shear zone, Kohistan, Pakistan. In M. H. Salisbury, & D. M. Fountain (Eds.), *Exposed cross-sections of the continental crust. NATO ASI series* (pp. 175–214). Springer Netherlands. https://doi.org/10.1007/978-94-009-0675-4_8

Treloar, P. J., Petterson, M. G., Jan, M. Q., & Sullivan, M. A. (1996). A re-evaluation of the stratigraphy and evolution of the Kohistan arc sequence, Pakistan Himalaya: Implications for magmatic and tectonic arc-building processes. *Journal of the Geological Society*, *153*(5), 681–693. https://doi.org/10.1144/gsjgs.153.5.0681

Ullah, M., Klötzli, U., Rentenberger, C., Sláma, J., Younas, M., Khubab, M., Goudarzi, M., & Ahmad, T. (2025). Unravelling the geochemical and geochronological diversities of the pre-collisional magmatism: Implications for the subduction dynamics in the Kohistan island arc and Karakorum block, Pakistan. *Geoscience Frontiers*, *16*(2), 102003. https://doi.org/10.1016/j.gsf.2025.102003

Zanchi, A., Poli, S., Fumagalli, P., & Gaetani, M. (2000). Mantle exhumation along the Tirich Mir fault zone, NW Pakistan: Pre-mid-cretaceous accretion of the Karakoram terrane to the Asian margin. *Geological Society, London, Special Publications*, *170*(1), 237–252. https://doi.org/10.1144/GSL.SP.2000.170.01.13